Nonlinear Inferential Control of Pulp Digesters

Jay H. Lee and A. K. Datta
Chemical Engineering Dept., Auburn University, Auburn, AL 36849

Monitoring and control of batch pulp digesters, which convert wood chips to pulp by Kraft process are discussed. The Kappa number, which represents the extent of delignification, is the key controlled variable, which cannot be measured on-line and must be estimated through secondary liquor measurements. Given a fixed batch time, the final Kappa number should be as close to the target Kappa number as possible, despite errors in the initial state estimates and input disturbances. To fulfill this objective, a state-observer-based model-predictive controller is designed using a detailed nonlinear dynamic model of the digester. The extended Kalman filter (EKF) using on-line measurements of various liquor characteristics is capable of recovering from significant errors in the initial state estimates. In addition, the EKF is shown to be robust to the errors in the covariance matrices and most model parameters, but quite sensitive to some model parameter errors. Coupled with the EKF, a finite-horizon model predictive controller (MPC) based on successive linearization of the nonlinear pulping model, is found to work efficiently for controlling the Kappa number and batch time.

Introduction

In a batch pulping unit, it is desired to achieve consistent pulp quality despite inconsistent feedstocks and changing operating conditions. Advanced controllers are implemented for pulp digesters to improve the uniformity of pulp quality, to reduce the production cost and to save energy (Dumont, 1986). Furthermore, if a proper level of delignification is not achieved during pulping, it necessitates more chemical consumption during bleaching of the pulp, leading to more toxic wastes.

Figure 1 shows a simple process diagram of a batch digester. Pulp digesters usually use the Kraft pulping process, in which an aqueous mixture of sodium hydroxide and sodium sulphide (called *white liquor*) is used to break away the lignin from cellulose fibers of wood, producing pulp of a desired Kappa number. Kappa number is a common measure of the residual lignin content in the pulp. In the batch process, the cooking reaction is stimulated by raising the digester temperature, which in turn is accomplished by either direct injection of steam or circulating a portion of the cooking liquor through an external heat exchanger. We will consider the latter method in this article: the temperature and the flow rate of the circulating liquor will be manipulated to control the Kappa number. Properties of feedstocks may vary from batch to batch, and in industry it is not possible to note the exact amount of such variations. An example of such variations would be types of woods used or proportion of two types of wood chips used as a mixture, both of which will alter wood compositions. Apart from this, there is also the possibility of unmeasured disturbances (due to errors in the transmitter signals and actuators) entering through the recirculation flow rate and temperature. The maximum allowed magnitudes and rates of change for inputs are usually limited by design or process considerations.

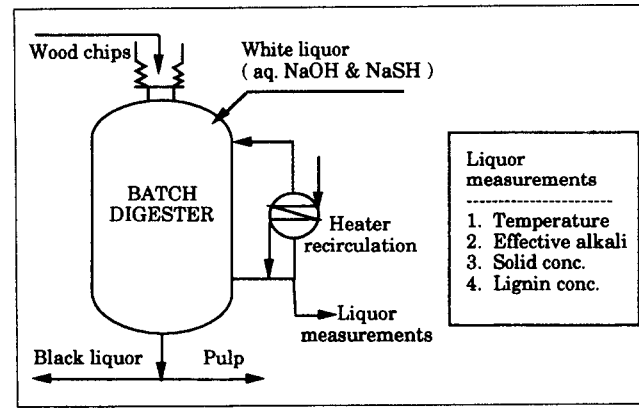

Figure 1. Batch pulp digester.

Correspondence concerning this article should be addressed to J. H. Lee.

For example, the maximum achievable temperature of the recirculation and its rate of change are limited by the design of the heater; similarly, the maximum flow rate of the recirculation is limited by the pumping capacity. The control objective is to monitor the Kappa number and to manipulate the inputs during the batch so that the Kappa number of pulp decreases in a desired fashion to its target value within a given batch time, despite various initial state uncertainties, disturbances, process constraints, and so on.

Two factors have impeded development of suitable on-line control techniques for pulp digesters: the lack of detailed understanding of the pulping phenomena and the inability to measure the Kappa number on-line. Even though pulping is an ancient method, many intricate details of its chemistry are still unknown, and a fundamental dynamic model is still in an evolving stage. In industry, control of a pulp digester relies mostly on manual adjustments of cooking temperature or on a controller based on various empirical models. Empirical models such as the Hatton's model (1973) or Chari's model (1973) can be used to adjust cooking temperature, based on feed-forward measurements obtained at the start of each batch. Feedback measurements of the Kappa number, which can be made only after pulp is withdrawn as product at the end of cooking, are also used in some control algorithms to modify model or controller parameters from time to time. Due to the inherent delay of single batch time for such measurements, however, it is impossible to account for the feedstock variations occurring from batch to batch. In addition, empirical parameters have to be reestimated each time when some major changes occur within the process. Some empirical models such as the Chari's model (1973), Kerr model (Kerr and Uprichard, 1976), or similar models (such as those proposed by Wells, 1990; Venkateswarlu and Gangiah, 1992) can use on-line measurements of effective alkali and temperature to adjust cooking temperature (and/or model parameters). However, while these strategies may work well in one case, they may fail elsewhere because of the empirical nature of these models. At present, researchers are focusing on developing semiempirical or fundamental models such as the Purdue model (Williams and Smith, 1975; Williams et al., 1984), static material balance models (Poulonis and Krishnagopalan, 1991), or statistically correlated models (Armstrong, 1991).

Since direct on-line measurement of the Kappa number is not possible (pulp cannot be taken out of the digester during cooking), the extent of delignification must be inferred from available *secondary* measurements. This difficulty is aggravated by the fact that accurate initial state estimates are often unavailable. This means that a model-based controller will not be successful unless these initial state errors are corrected by a state observer. In the past, the only liquor measurements utilized for control were those of the liquor temperature and effective alkali. However, these two measurements alone are unlikely to provide sufficient information to recover from significant initial state errors within reasonable time. Recently, new liquor analyzers have been developed to obtain more properties of the Kraft liquor (such as liquor lignin concentration, solid concentration). Since these properties depend on the extent of reaction, they provide us with additional information on how the pulping progresses in real time. Therefore, these new measurement techniques have opened the door for design of a more efficient Kappa number estimator. Among various nonlinear estimation techniques, the extended Kalman filter (EKF) (Kopp and Oxford, 1963; Cox, 1987b) has been the most popular choice. The EKF requires much less on-line computation than other more rigorous estimation methods using nonlinear optimization. In control literature, good convergence properties of EKF in estimating not only the states but also model parameters have been reported for a number of chemical and biochemical systems, many of which are reaction systems similar to the pulp digester (Bellgardt et al., 1986; Corcoran and Rutan, 1988; Myers and Luecke, 1991; Wells, 1971). If designed properly, the EKF is expected to yield good estimates for most batch processes, provided sufficient measurements are available.

Control of a batch digester is inevitably a nonlinear control problem. Because most chemical processes are highly nonlinear and many of them need to be operated over a wide range, the topic of nonlinear control has received much attention lately, from theoreticians and practitioners alike. A wide array of nonlinear control techniques are available these days, ranging from simple gain scheduling of linear controllers to more rigorous nonlinear techniques such as the differential-geometry-based approach and nonlinear model predictive control (NLMPC or NMPC) (Bequette, 1991). Among these techniques, particularly NLMPC has been drawing considerable interest from industry, owing largely to its ability to address many practical issues (such as process constraints) in a unified framework. Two approaches to the nonlinear model predictive control can be envisaged: gain scheduling and nonlinear optimization. The main idea of the first approach is to transform the nonlinear system into a time-varying linear system so that the standard linear MPC technique can be applied. In the second approach, setpoint tracking error minimization is formulated as a nonlinear programming (NLP) problem by discretizing the model differential equations (Beigler and Cuthrell, 1987; Rawlings et al., 1990). High numerical complexity and computational requirement have thus far prevented practical implementation of the method.

Among the gain scheduling techniques, the successive linearization approach stands out as a well-accepted choice as it represents a good compromise between the theoretical rigor and computational efficiency. Garcia (1984) first proposed nonlinear quadratic dynamic matrix control (NLQDMC), in which the future output behavior is predicted by integrating the nonlinear model differential equation while holding all the inputs constant at the values corresponding to the previous time step. The effect of future input moves is then estimated, based on the model *linearized* at the current state estimates and added. To account for unmeasured disturbances and other state errors, a bias term (corresponding to the difference between the measurement and the estimated output) is added uniformly to the predicted output. The use of the open-loop state estimator, as well as the bias measurement update step in this method, is somewhat heuristic, but he showed good results in applying the technique to a polymerization process. Recently, Gattu and Zafiriou (1992) extended NLQDMC to unstable processes by incorporating the steady-state Kalman filter, which is redesigned at each time step based on the locally linearized model. This method combines the closed-loop observer with an open-loop disturbance estimator in a heuristic manner and does not build state estimates of the *true* states; therefore, it is not suitable for inferential control problems.

More recently, Lee and Ricker (1993) proposed a similar technique, based on the Extended Kalman filter. In their approach, physical state disturbances are modeled as appropriate nonstationary stochastic processes, and the EKF is used to construct the estimates for the true states. Future outputs are predicted by integrating the nonlinear model with the current state estimates, using the local linear approximation for computing the effect of future input moves. The technique is expected to work well for inferential control, since it estimates the "true" states by modeling the initial errors and physical disturbances as appropriate stochastic variables.

This article presents an application study of the EKF-based NLMPC technique to the outlined batch pulp digester problem, taking advantage of the measurements from the new liquor analyzers. Its purpose is to assess the feasibility and potential benefits of using such advanced sensor and control techniques for pulp digester control and to investigate the required model accuracy for successful application. The study is based on a simulator developed using a fundamental kinetic model. The ability of the EKF to converge to the true Kappa number in the presence of significant unmeasured initial state errors and disturbances is examined, as well as the effect of various on-line liquor measurements on the quality of state estimation. While the estimate from the EKF using the conventional liquor measurements alone fails to converge to the true Kappa number within reasonable time, the additional liquor measurements provided by the new sensors speed up the convergence dramatically. The successive linearization-based MPC is shown to control the batch time efficiently, given that the Kappa number estimate converges to its true value sufficiently early. Finally, our study shows that the EKF-based MPC is quite robust to the errors in most of the model/design parameters, but is sensitive to certain sets of model parameters like the activation energies of the reaction.

Control difficulties addressed here are common among other control problems of industry. The proposed nonlinear control algorithm is of manageable computational complexity and therefore is applicable to a broad range of control problems at the present time. To enhance the tutorial value of the article, less emphasis is given to the theoretical aspects of the technique and the focus is on the implementational aspects, such as the formulation of physical issues within the given theoretical framework, choice of tuning parameters, and step-by-step implementation of the algorithm.

Formulation of Model and Control Problem

In this section, we describe the dynamic model, as well as the states, outputs, inputs and disturbances of the pulp digester. We also show how to obtain an augmented form of the discretized process and disturbance models. Our model is adopted from (Williams and Smith, 1975; Williams et al., 1984) who first applied the complex chemistry of pulping in a simple fashion and developed the kinetic model for wood components undergoing the reaction. The resulting model is based on the mass and energy balances for the three phases of the reaction mixture: wood or pulp, entrapped liquor (residing within the pores of wood or pulp), and free or bulk liquor phases. The 14 coupled ordinary differential equations detailed in Appendix A can be written in the following standard state-space form:

$$\dot{x} = f(x, u, d) \tag{1}$$

$$y^c = Hx + H^d d \tag{2}$$

$$\hat{y} = g(x, d) + \nu \tag{3}$$

where f and g represent the nonlinear relationships expressed in the model equations, and x, y^c, y, u, d, and ν are vectors containing states, controlled outputs, measured outputs, manipulated inputs, unmeasured disturbances and output noises, respectively. The notion $\hat{}$ for y is used to emphasize the fact that the measured outputs are corrupted by noise. For simplicity, it is assumed that the controlled variables are linear combinations of states and disturbances. The specific elements of the above vectors are discussed below.

States

The state vector consists of 14 variables including five wood compositions, four entrapped liquor compositions, four free liquor compositions, and temperature:

$$x = [X_1 \cdots X_5 C_{e_1} \cdots C_{e_4} C_{f_1} \cdots C_{f_4} T]^T \tag{4}$$

Controlled output

The controlled variable y^c for pulping is the Kappa number ($\mathcal{K}$), which is defined as (Williams and Smith, 1975):

$$\mathcal{K} = 653.6(X_1 + X_2) \tag{5}$$

where $(X_1 + X_2)$ represent the total lignin concentration in the pulp.

Measured output

The usual on-line measured outputs consist of the temperature (T) and effective alkali ($\mathcal{E}$) of the free liquor. Effective alkali in free liquor is defined as:

$$\mathcal{E} = C_{f_3} \frac{62.0}{80.0} \tag{6}$$

It represents the net amount of Na_2O present as NaOH in the free liquor. The effective alkali can be determined from the measurement of the conductivity of the liquor. Recently, a novel on-line sensor technique has been developed at Auburn University, enabling the real-time estimation of not only the temperature and effective alkali, but also the total solid concentration (S_f) and lignin concentration (L_f) of the cooking liquor (Poulonis and Krishnagopalan, 1991). These outputs can be determined from the measurements of UV absorption and refractive index of the liquor. Liquor lignin concentration is due to all types of lignin from wood, and liquor solid concentration is due to all types of dissolved components from wood including the lignin:

$$L_f = C_{f_1} \tag{7}$$

$$S_f = C_{f_1} + C_{f_2} \tag{8}$$

The measured output vector can be written as:

$$y=[T\ \mathcal{E}\ S_f\ L_f]^T \tag{9}$$

In some cases studies presented here, we will use only a subset of the four measurements to evaluate the benefits of using particular measurements.

Manipulated inputs

The manipulated variables consist of the recirculation temperature and flow rate:

$$u=\begin{bmatrix} T_r \\ F_r \end{bmatrix} \tag{10}$$

These variables are controlled by the lower-level loops, the set points of which are to be provided by the Kappa number control system.

Unmeasured disturbances and output noises

Measurements are inevitably corrupted by noise, and the noise effect needs to be considered in analyzing and designing a control system. In general, measurement noises are modeled adequately as zero-mean random variables (such as white noise). The covariances of these random variables are often unknown and must be regarded as parameters to be adjusted through simulation and/or on-line tuning.

Knowledge of sources and nature of disturbances is quite limited in most cases. Unmeasured disturbances can enter a process through unexpected variations in external inputs. For state estimation, disturbances are usually modeled as stochastic processes of the form:

$$x_k^w=A^w x_{k-1}^w+B^w w_{k-1} \tag{11}$$

$$d_k=C^w x_k^w \tag{12}$$

where w_k is white noise. The knowledge of the disturbance characteristics, as well as their intensity and frequency, is utilized in choosing the disturbance model parameters A^w, B^w, and C^w, as well as the covariance matrix for w_k.

For the batch pulp digester, the only plausible unmeasured disturbances (besides the feedstock variations that are better expressed as initial state estimate errors) are the discrepancies between the controller-specified setpoints and actual values of the manipulated inputs, caused by transmitter/actuator errors in the lower-level loops. We use the knowledge that such disturbances are likely to change in a random walk fashion:

$$d_{k+1}=d_k+w_k \tag{13}$$

where d_k and w_k represent the integrated and ordinary white noises at time k. Equation 13 can be expressed in the standard form of Eq. 11 as:

$$x_{k+1}^w=\begin{bmatrix} 1 & 0 \\ 0 & 1 \end{bmatrix} x_k^w+\begin{bmatrix} 1 & 0 \\ 0 & 1 \end{bmatrix} w_k \tag{14}$$

$$d_k \triangleq \begin{bmatrix} d_{1_k} \\ d_{2_k} \end{bmatrix}=\begin{bmatrix} 1 & 0 \\ 0 & 1 \end{bmatrix} x_k^w \tag{15}$$

d_{1_k} and d_{2_k} are the unmeasured disturbances to be added to the controller outputs (setpoints for the recirculation temperature and flow rate, respectively) to represent the actual values of these variables:

$$\begin{bmatrix} T_r \\ F_r \end{bmatrix}=\begin{bmatrix} T_r^s \\ F_r^s \end{bmatrix}+\begin{bmatrix} d_{1_k} \\ d_{2_k} \end{bmatrix} \tag{16}$$

where T_r^s and F_r^s are the setpoints for T_r and F_r provided by the Kappa number controller. Again, the covariance matrix of w_k is difficult to estimate *a priori* and is better determined through simulation or on-line tuning.

Assuming zero-order hold and the sampling time of T_s, a discrete form of the model (Eqs. 1-3) is given by:

$$x_k=f_{T_s}(x_{k-1},\ u_{k-1},\ d_{k-1}) \tag{17}$$

$$y_k^c=Hx_k+H^d d_k \tag{18}$$

$$\hat{y}_k=g(x_k,\ d_k)+v_k \tag{19}$$

where $k=1$, 2, and so on is the index for the discrete time sequence and $f_{T_s}(x_{k-1},\ u_{k-1},\ d_{k-1})$ is the state vector obtained by integrating the model (Eq. 1) for one sampling interval with initial condition x_{k-1} and constant inputs u_{k-1} and d_{k-1}.

Combining the process model (Eqs. 17-19) with the disturbance model (Eqs. 11-12), we arrive at the following augmented model:

$$\begin{bmatrix} x_k \\ x_k^w \end{bmatrix}=\begin{bmatrix} f_{T_s}(x_{k-1},\ u_{k-1},\ C^w x_{k-1}^w) \\ A^w x_{k-1}^w \end{bmatrix}+\begin{bmatrix} 0 \\ B^w \end{bmatrix} w_{k-1} \tag{20}$$

$$y_k^c=Hx_k+H^d d_k \tag{21}$$

$$\hat{y}_k=g(x_k,\ C^w x_k^w)+v_k \tag{22}$$

This model will be the basis of our further discussion.

Extended-Kalman-Filter-Based Nonlinear Model Predictive Control

In this section, the EKF-based NLMPC technique proposed by Lee and Ricker (1993) is reviewed briefly. The step-by-step procedure for implementation is as follows.

Step 1: initiation

Set the time index to zero: $k=0$. Start with the initial values of inputs u_0, estimates of the states $x_{0|0}$ and disturbance states $x_{0|0}^w$. The notation $\{\cdot\}_{k|\ell}$ represents the estimated value of a vector or matrix at time k based on measurements up to time ℓ.

Choose the initial covariance matrices required to run the EKF, namely, the covariances of the error between the estimated and true values of the states ($\Sigma_{0|0}$), of the state noise (R^w) and of the measurement noise R^v. $\Sigma_{0|0}$ should be chosen according to the expected magnitudes of the errors in the state

estimates as well as any known correlations among them. R^w and R^v can be selected based on the expected magnitudes of various disturbances and noise. These matrices have strong influence on the quality of estimation, and their values may need to be retuned further after implementation. Select controller parameters such as the size of the prediction horizon (p), number of control moves (m) to be computed each time, and weighting matrices for the outputs (Λ^y) and inputs (Λ^u) for the optimization objective. Note that Λ^y and Λ^u are usually chosen as diagonal matrices, and m may be specified to be less than p. Like the EKF, MPC parameters may require further tuning to yield the best results. Also determine effective constraints for various inputs and outputs, and the future reference values of the controlled outputs.

Step 2: model update

Set $k=k+1$. Update the states by integrating the nonlinear model (Eq. 1) with the initial conditions $x_{k-1|k-1}$ and constant inputs u_{k-1} and $C^w x^w_{k-1|k-1}$.
State:

$$\begin{bmatrix} x_{k|k-1} \\ x^w_{k|k-1} \end{bmatrix} \approx \begin{bmatrix} f_{T_s}(x_{k-1|k-1},\, u_{k-1},\, C^w x^w_{k-1|k-1}) \\ A^w x^w_{k-1|k-1} \end{bmatrix} \tag{23}$$

Also update the state error covariance matrix as follows:
State Error Covariance:

$$\Sigma_{k|k-1} = \Phi_{k-1}\Sigma_{k-1|k-1}\Phi^T_{k-1} + \Gamma^w R^w (\Gamma^w)^T \tag{24}$$

Φ_{k-1} and Γ^w are given by:

$$\Phi_{k-1} = \begin{bmatrix} A_{k-1} & B^d_{k-1} C^w \\ 0 & A^w \end{bmatrix} \tag{25}$$

$$\Gamma^w = \begin{bmatrix} 0 \\ B^w \end{bmatrix} \tag{26}$$

Matrices A_{k-1} and B^d_{k-1} are obtained through linearization and discretization of Eq. 1 with respect to $(x_{k-1|k-1},\, u_{k-1},\, C^w x^w_{k-1})$; their definitions are in Appendix B.

Step 3: measurement corrections

Correct the state estimates using the current measured output $\hat{y}_k$:
State:

$$\begin{bmatrix} x_{k|k} \\ x^w_{k|k} \end{bmatrix} = \begin{bmatrix} x_{k|k-1} \\ x^w_{k|k-1} \end{bmatrix} + L_k\{\hat{y}_k - g(x_{k|k-1},\, C^w x^w_{k|k-1})\} \tag{27}$$

In Eq. 27, L_k is the Kalman filter gain given by:

$$L_k = \Sigma_{k|k-1}\Xi^T_k (\Xi_k \cdot \Sigma_{k|k-1}\Xi^T_k + R^v)^{-1} \tag{28}$$

where

$$\Xi_k = [C_k C^d_k C^w]^T \tag{29}$$

C_k and C^d_k are obtained by linearizing the output equation (see Appendix B for definition). The state error covariance matrix $\Sigma_{k|k-1}$ also needs to be updated accordingly.
State Error Covariance:

$$\Sigma_{k|k} = [I - L_k \Xi_k]\Sigma_{k|k-1} \tag{30}$$

Step 4: output prediction

The optimal prediction of the controlled outputs (y^c) for p future time steps using the local linear approximation of the model can be written as:

$$\begin{aligned} \mathcal{Y}_{k+1|k} &= \mathcal{S}^x_k(x_{k|k},\, u_{k-1},\, x^w_{k|k}) + S^w_k x^w_{k|k} + S^{\mathcal{U}}_k \Delta\mathcal{U}_k \\ &\triangleq \mathcal{Y}^0_{k+1|k} + S^{\mathcal{U}}_k \Delta\mathcal{U}_k \end{aligned} \tag{31}$$

where

$$\mathcal{Y}_{k+1|k} = \begin{bmatrix} y^c_{k+1|k} \\ y^c_{k+2|k} \\ \vdots \\ y^c_{k+p|k} \end{bmatrix};\quad \Delta\mathcal{U}_k = \begin{bmatrix} \Delta u_k \\ \Delta u_{k+1} \\ \vdots \\ \Delta u_{k+p-1} \end{bmatrix} \tag{32}$$

$S^x_k(x_{k|k},\, u_{k-1},\, x^w_{k|k})$ is the vector of future outputs obtained by integrating the nonlinear model equation (Eq. 1) with the assumption of no change in the inputs and disturbance trends. S^w_k and $S^{\mathcal{U}}_k$ are constant matrices constructed from various Jacobian matrices (obtained via local linearization) and reflect the effect of current disturbances and future input changes on the controlled variables, respectively. Hence, in this step, the vector $S^x_k(x_{k|k},\, u_{k-1},\, x^w_{k|k})$ and matrices S^w_k, $S^{\mathcal{U}}_k$ need to be constructed by performing nonlinear integration and local linearization, respectively. The exact definitions for these vector and matrices can be found in Appendix B.

Step 5: control move computation

Find a sequence of m control moves that minimizes the following objective:

$$\min_{\Delta\mathcal{U}_k} \|\Lambda^y(\mathcal{Y}_{k+1|k} - \mathcal{R}_{k+1|k})\|^2_2 + \|\Lambda^u \Delta\mathcal{U}_k\|^2_2 \tag{33}$$

such that

$$\Delta u_{k+m} = \cdots = \Delta u_{k+p-1} = 0. \tag{34}$$

$$u^{\text{low}}_{k+l} \le u_{k+l} \le u^{\text{high}}_{k+l},\quad 0 \le l \le m-1 \tag{35}$$

$$-\Delta u^{\max}_{k+l} \le \Delta u_{k+l} \le \Delta u^{\max}_{k+l},\quad 0 \le l \le m-1 \tag{36}$$

$$y^{\text{low}}_{k+l} \le y_{k+l} \le y^{\text{high}}_{k+l},\quad 1 \le l \le p \tag{37}$$

where $\mathcal{R}_{k+1|k} = [r^T_{k+1|k} \cdots r^T_{k+p|k}]^T$ is a vector containing future reference values. Because prediction equation (Eq. 31) is linear in $\Delta\mathcal{U}_k$, the above optimization can be solved via standard quadratic programming.

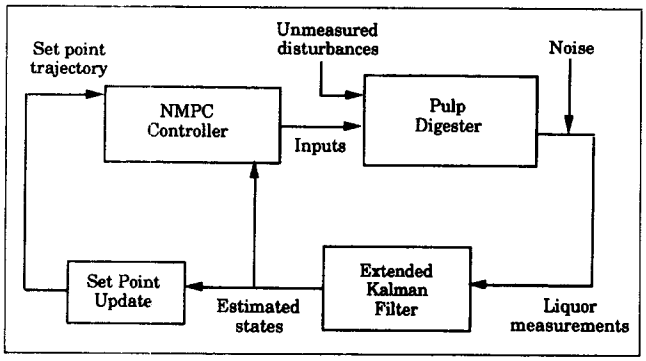

Figure 2. State estimation based NLMPC (or NMPC) controller.

Step 6: implementation and continuation

Implement the first element of the calculated control moves $\Delta\mathfrak{U}_k$: $u_k = u_{k-1} + \Delta u_k$. If control is to be continued to the next time step, go back to step 2.

Application of EKF-Based NLMPC to Batch Digester

Our objective, as already mentioned, is to monitor the pulp Kappa number and control the batch time, in the presence of errors in the initial state estimates and unmeasured input disturbances. Unlike many other industrial reactions, pulping is a slow reaction process requiring a few hours to complete. This means that changes in the state variables will be small over a typical sampling interval (of three minutes or so). Hence, the local linearization-based NLMPC technique is expected to yield adequate state estimates and control.

To ensure stability and convergence of the EKF, on-line measurements carrying information on the states of the model must be available. For inferential control problems, states constituting the controlled outputs are not reflected directly in the measured outputs. In many cases, however, the time sequence of the measured outputs can provide sufficient amount of information for estimating the controlled variables (this condition is called "observability" in control parlance). Newly developed on-line analyzers, like those measuring the lignin and solid concentrations in the free liquor, can provide valuable information based on which the progress of the pulping reaction can be followed in real time. Such measurements, being closely related to the delignification and dissolution of wood, are more useful for estimating the Kappa number than the temperature and effective alkali measurements.

Figure 2 shows the extended-Kalman-filter-based nonlinear model predictive controller applied to the batch digester control problem. Further discussions of the model and plant data used, design of the state estimator, design of the controller, selection

Table 1. Initial States and Errors Used for Various Case Studies

States	True Values	Initial Errors (1A to 1D & 2)* Type 1	Initial Errors (1A to 1D & 2)* Type 2	Initial Errors (1E only)*	Noise Intensities (1D only)**
X_1 = high-reactive lignin conc. (mass fraction in wood)	0.0528	−0.01	0.01	±0.02†	0.0005
X_2 = low-reactive lignin conc. (mass fraction in wood)	0.2112	−0.05	0.05	±0.08	0.002
X_3 = cellulose conc. (mass fraction in wood)	0.4852	−0.02	0.02	±0.10	0.005
X_4 = galactoglucomannan conc. (mass fraction in wood)	0.1428	−0.02	0.02	±0.05	0.001
X_5 = araboxylan conc. (mass fraction in wood)	0.0722	−0.01	0.01	±0.03	0.0007
C_{e_1} = total lignin conc. (kg/m³ in entrapped liquor)	0	0	0	0	0.3
C_{e_2} = total solid conc. (kg/m³ in entrapped liquor)	0	0	0	0	0.5
C_{e_3} = NaOH conc. (kg/m³ in entrapped liquor)	0	0	0	0	0.2
C_{e_4} = NaSH conc. (kg/m³ in entrapped liquor)	0	0	0	0	0.02
C_{f_1} = total lignin conc. (kg/m³ in free liquor)	1 (2)‡	−1	−1	−2	0.3
C_{f_2} = total solid conc. (kg/m³ in free liquor)	2 (3)‡	−2	−2	−3	0.5
C_{f_3} = NaOH conc. (kg/m³ in free liquor)	47.6327	−3	3	±4	0.2
C_{f_4} = NaSH conc. (kg/m³ in free liquor)	11.3535	−2	2	±3	0.02
T = temperature (°C)	80	−1	1	±2	1

*1A to 1E & 2 represent various case studies.
**White noises of these intensities are added to each state for case study 1D.
†"−" & "+" signs stand for type-1 & type-2 initial errors respectively.
‡Higher values are used in case study 1D, since in this case study errors are larger but estimates remain the same as other case studies.

Table 2. Operating Conditions Used for Simulation

Operating Conditions	Values
Initial dry wood mass (kg)	100
Dimensions of wood chip (m)	$0.08 \times 0.08 \times 0.005$
Porosity of wood chip	0.5
Dry wood density (kg/m^3)	425
Initial white liquor volume (m^3)	0.35
Initial Kappa number	172.5
Target Kappa number	49
Cooking time (h)	2
Sampling time (h)	0.05

of the process constraints, and choice of the setpoint trajectory in the context of Lee and Ricker's technique are given next.

Model and plant data

Most of the plant and model data are presented by Williams et al. (1982, 1987). Table 1 includes true initial values of the 14 states, errors introduced to the estimates of these true initial states for different case studies. The initial state errors (types 1 and 2) used in our simulation represent only two of infinitely many possible sets of errors. There is no specific reason for the choice of errors; however, it may be noted that these two types of errors are of opposite signs. By introducing these errors to the initial state estimates, we examine how well the extended Kalman filter recovers from them.

Other initial conditions and operating data used are given in Table 2. Data for the model parameters are shown in Table 3. A sampling time of 3 min is used since it is the minimum time required presently to collect and analyze all the four measurements.

To assess the performance of the estimator, the estimated output is compared with the actual plant output. Actual plant outputs are generated by integrating the model equations with the true values of the states and parameters. Zero-mean random variables, each of unit variance, are added to the plant outputs to simulate the measurement noise (v). Furthermore, unmeasured disturbances (d) entering the recirculation temperature and flow rate were simulated as random walk processes generated by integrating the white noises (w) of covariances $4.0e-02$ and $9.0e-06$, respectively.

State estimator design

State estimation is made using the recursive EKF algorithm in steps 2 and 3. Performance of the EKF is affected by the choice of various design parameters including the initial state-error covariance matrix $\Sigma_{0|0}$, the state-noise covariance matrix R^w, and the output-noise covariance matrix R^v. These matrices are to be chosen according to the expected magnitudes (and frequencies) of the stochastic signals. $\Sigma_{0|0}$ is usually chosen as a diagonal matrix unless one has *a priori* knowledge on the correlations among the errors in different states. Each diagonal element is set in proportion to the square of the expected error in the estimate of the corresponding state variable. The choice of R^w and R^v should also reflect the statistical average of the changes in the unmeasured disturbances and magnitudes of the output noises, respectively. More often, however, these covariance matrices are chosen heuristically and are further adjusted on-line for the best performance. In general, large values in $\Sigma_{0|0}$ and R^w increase the speed of update, but raises the sensitivity to measurement noise and model errors. Large values in R^v have the opposite effect.

With these guidelines and after some fine-tuning, we ended up with the covariance matrices shown in Table 4. $\Sigma_{0|0}$ was

Table 3. Model Parameters Used for Simulation

Parameters	Values
A_{1_i} = first frequency factors for five wood components (h^{-1} $(kg/m^3)^{-1}$)	19.41, 4.16e+12, 445.12, 108.00, 7.05e+05
A_{2_i} = second frequency factor for five wood components (h^{-1} $(kg/m^3)^{-a-b}$)	7.00e+03, 2.75e+04, 8.30e+03, 6.00e+03, 1.75e+04
E_{1_i} = first activation energy for five wood components (kcal/mol)	639.28, 33.77, 1.94e+03, 717.94, 3.95e+18
E_{2_i} = second activation energy for five wood components (kcal/mol)	7.50e+03, 9.00e+03, 1.00e+04, 9.00e+03, 4.0e+04
a = reaction order w.r.t. NaOH	0.5
b = reaction order w.r.t. NaSH	0.5
X_{u_i} = conc. of unreactive wood components (mass fraction)	0, 0, 0.71, 0.25, 0
$S_{c_{3_j}}$ = stoichiometric coefficient of NaOH for five wood components (kg/kg)	0.166, 0.166, 0.395, 0.395, 0.395
$S_{c_{4_j}}$ = stoichiometric coefficient of NaOH for five wood components (kg/kg)	0.0546, 0.0546, 0, 0, 0
M_{1_i} = first constant in mass-transfer coeff. equation (m/h)	−0.06
M_{2_i} = second constant in mass-transfer coeff. equation (m/h·K)	2.0e−04
ΔH_i = heat of reaction, for all components (kcal/kg wood component reacted)	102.8
Cp_{w_i} = specific heat of wood components (kcal/(kg·K)) for all components	0.36

Table 4. Tuning Parameters and Process Constraints Used in the Controller Algorithm

Estimator Tuning Matrices	Values
Initial state error covariance (Σ_{010})	diag ([1.0e−04, 2.5e−03, 4.0e−04, 4.0e−04, 1.0e−04, 0, 0, 0, 0, 1, 4, 9, 4, 1])
Measurement noise covariance (R^v)	diag ([1, 1, 10, 5])
State noise covariance (R^w)	diag ([1.0e−04, 1.0e−06])
Controller Tuning Factors	**Values**
No. of prediction horizons (p)	10
No. of control moves (m)	10
Output weighing matrix (Λ^y)	diag ([1])
Input weighing matrix (Λ^u)	diag ([1.0e−06 1.0e−06])
Constraints	**Values**
Max. recirculation temp. ($T_{r_{max}}$)	250°C
Min. recirculation temp. ($T_{r_{min}}$)	Digester temperature in °C
Max. recirculation flow ($F_{r_{max}}$)	0.5 m^3/h
Min. recirculation flow ($F_{r_{min}}$)	1 m^3/h
Max. temperature change ($\Delta T_{r_{max}}$) per sampling time	10°C
Max. flow rate change ($\Delta F_{r_{max}}$) per sampling time	0.1 m^3/h

chosen to be commensurate with the initial state errors in Table 1. In selecting R^v, it was found that the state estimates were very sensitive to noises in the solid and lignin concentration measurements. Furthermore, noises in the solid concentration measurements were found to influence the filter performance more than noises in the lignin concentration measurements. Various covariance values were tried for the solid and lignin concentrations, before making the particular choice. In selecting R^w, it was assumed that the state noises enter only through the disturbance states x^w; noise models for the other states were assumed to be unknown or nonexistent. The covariances of white noises entering x^w were chosen according to the expected errors (deviation from the controller-specified setpoints) in the manipulated variables.

Model predictive controller design

Control moves are calculated by minimizing the quadratic objective function in Eqs. 33-37, utilizing the output prediction equations (Eqs. 31-32). The MPC controller requires choosing several tuning parameters: the size of prediction horizon (p), the number of input moves computed each time (m), output weighting factor (Λ^y) and input weighting factor (Λ^u). Elements of Λ^y are selected on the basis of their relative importance with respect to the others. Selection of the elements in Λ^u is based on two factors: 1. one should consider the relative importance of the input move minimization (and therefore robustness) with respect to the setpoint error minimization; 2. among various inputs, one may decide which one should vary more slowly than others. While tuning p and m, note that increasing p generally leads to more robust control at the cost of more computation. For batch process requiring the end-time control, a large prediction horizon may be preferable. It should, however, also be noted that the linearized model may alter considerably between sampling times, in which case too large a prediction horizon may not be helpful. Provided enough computing capability exists, setting m equal or near to p leads to more aggressive control action and tends to improve the overall performance in the presence of active constraints.

With these guidelines and after some tuning, parameters in Table 4 are chosen. Since the Kappa number is the only controlled output (y^c) and there are two manipulated inputs (u), Λ^y contains only a single parameter and Λ^u contains two parameters. Without loss of generality, Λ^y was set at unity and the other two parameters for Λ^u were adjusted. Very small values were found to work well for these two parameters, because the input constraints were set tightly enough to provide smooth, robust control moves. The reason for choosing the prediction horizon p and number of control moves m as 10 is that lower values of p and m resulted in inferior performance, while increasing them further did not lead to any noticeable improvement.

Process Constraints. Process constraints, that can be incorporated into the MPC algorithm, may vary widely from one pulping plant to another. Typical data in the literature only mention the constraints for the cooking temperature, which is usually in the range of 160 to 180°C. We assigned the maximum value of the recirculation temperature to be somewhat higher than this range. Since no cooling can be done beyond the existing temperature inside the digester, this gives us a lower bound of the recirculation temperature. Constraints on the recirculation flow rate were chosen according to our physical intuition, considering the digester capacity (free liquor volume). Finally, the rate constraints of both inputs were also chosen according to our physical intuition. Values of the input constraints incorporated into the algorithm are shown in Table 4. We did not impose any output constraint in the algorithm.

Set-Point Trajectory. In specifying the reference trajectory of the Kappa number for MPC, we examined two options: using a prespecified trajectory and updating it at each time step based on the current estimate of the Kappa number. The first option was found to work inadequately leaving offset at

the end since the proper Kappa number trajectory depends on the true initial conditions which are unknown. For the second option, because the reference trajectory is updated at each sampling time and we are using a relatively short prediction horizon compared to the batch time, a linear trajectory calculated in the following manner was found to be adequate:

$$r_{k+\ell|k} = \mathcal{K}_{k|k} - \ell \frac{\mathcal{K}_{k|k} - \mathcal{K}_f}{(t_f - t_k)/t_s} \tag{38}$$

where $r_{k+\ell|k}$ is the current setpoint for the Kappa number at time $k+\ell$, $\mathcal{K}_{k|k}$ the estimated value of the current Kappa number, and $\mathcal{K}_f$ the target Kappa number, t_k, t_f and t_s represent the current time, final batch time, and sampling interval, respectively.

Results and Discussions

We used MATLAB/SIMULINK for dynamic simulation and MPC calculation. The performance of the controller is judged by how close the final Kappa number is to the target Kappa number for a fixed batch time. For assessing the efficiency of the EKF, we note how fast the estimated Kappa number converges to the true value. Note that although simulations have been performed for all the following case studies with both types of initial errors, due to the space limitation, we present here only some of the results.

Case study 1

In the first case study, we will compare results for the following cases:

Case 1A. No measurement is used for state estimation (open-loop control).

Case 1B. Measurements of the temperature and effective alkali are used for state estimation.

Case 1C. All four measurements, lignin and total solid concentrations, effective alkali and temperature, are used for state estimation.

Case 1D. All four measurements are used for state estimation, but actual states are disturbed by random noises which have not been considered in the assumed model of unmeasured disturbances. In other words, the true states are calculated as:

$$\dot{x} = f(x, u, d) + w_u \tag{39}$$

where w_u is unmodeled white noise. Table 1 shows the intensities of such unmodeled state noise used for the simulation. Physically, such random noise may account for additional state errors caused by model errors or unmodeled disturbances.

Case 1E. All four measurements are used for state estimation, but much larger errors are present in the initial state estimates than reflected by Σ_{010}. Table 1 shows the errors used in this case study.

Figure 3 shows how the estimated Kappa number profile differs from the true profile in case 1A for a particular type of initial state errors (such as type 1). Figures 4, 5, 6 and 7 show similar plots for case 1B (type 2 initial errors), case 1C (both types 1 and 2 initial errors), case 1D (type 1 initial errors) and case 1E (type 2 initial errors), respectively. The following observations can be made from these plots:

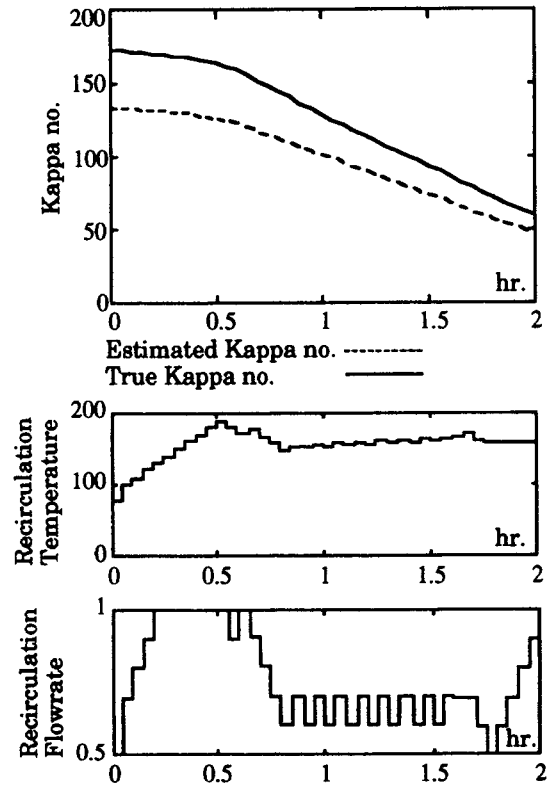

Figure 3. Case study 1A with type-1 initial state errors, when no measurement is used.

- Open-loop control (case 1A) results in a large offset in the Kappa number estimate, and we are left with undercooked or overcooked pulp.
- In going from case 1A to case 1B, use of the effective alkali and temperature measurements results in significant improvement. Initial errors, however, are not fully recovered until near the end of the batch time, and accurate control of the Kappa number and batch time is not achieved. Therefore, effective alkali and temperature measurements alone are insufficient for efficient recovery from significant errors in the initial state estimates. This is expected since, as already mentioned, the effective alkali and temperature measurements are not related strongly to the delignification rate and therefore they do not carry enough information to recover the true value of the Kappa number within a short period of time.
- In case 1C, estimation improves dramatically. The estimated Kappa number converges to the true value faster than the earlier cases and reaches the target value accurately at the end of the scheduled batch time. In addition to the lignin concentration, other states (not shown here) approach their true values, with very little residual errors. Clearly this has been made possible by the additional liquor lignin and solid concentration measurements, which are more closely related to the delignification of wood than the effective alkali and temperature measurements. Hence, they are critical for the performance of the Extended Kalman filter.
- In case 1D, we find that the state noise unaccounted for in the Kalman filter design has some effect on the quality of the estimation, but the estimates still recover quite efficiently.

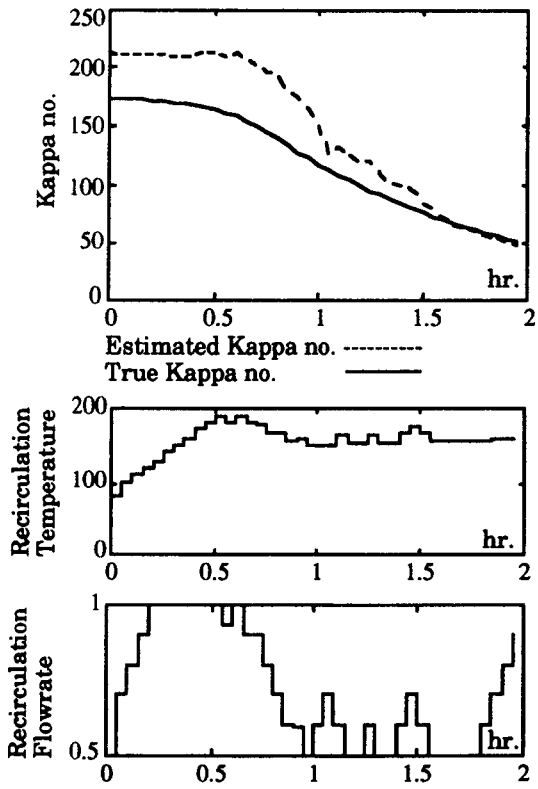

Figure 4. Case study 1B with type-2 initial state errors, closed-loop plot of estimated and true Kappa number profiles when two measurements are used.

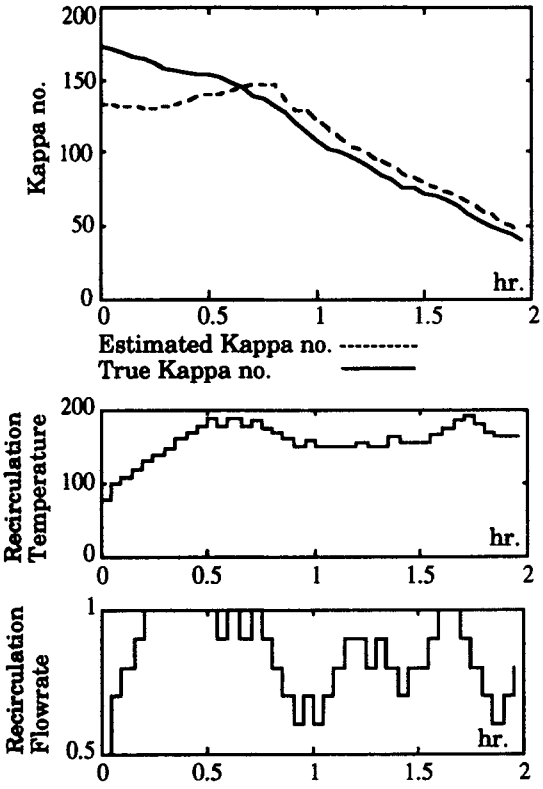

Figure 6. Case study 1D with type-1 initial state errors, effect of unmodeled state noise on the closed-loop profiles of the estimated and true Kappa number.

Some offset observed at the end can be attributed to the state noise that perturb the states continuously and is not due to the initial errors.

- From results of case 1E, we observe that significantly underestimated initial covariance matrix leads to only small degradation in the estimation quality.

The above observations can be corroborated by analyzing the system dynamic properties such as the *detectability*. Detectability implies that all unstable modes of the system are reflected in the measurements and is required for convergence of the estimates. In analyzing the detectability of the linearized system for each time step, it was found that, when we use all the four liquor measurements, the system remains detectable essentially for all the time steps. But with less than four measurements, such as effective alkali and temperature measurements only, the same observation does not hold. Therefore, we conclude that, whereas we can expect to recover from the initial errors in state estimates efficiently using all the four liquor measurements, the same may not be true with the effective alkali and temperature measurements only.

From this case study, we conclude that reliable control of a batch digester is possible when all the four liquor measurements are used for the extended Kalman filter. We can expect the controller to work adequately, even when the initial state error (or state noise covariances) is not chosen to reflect the physical situation exactly.

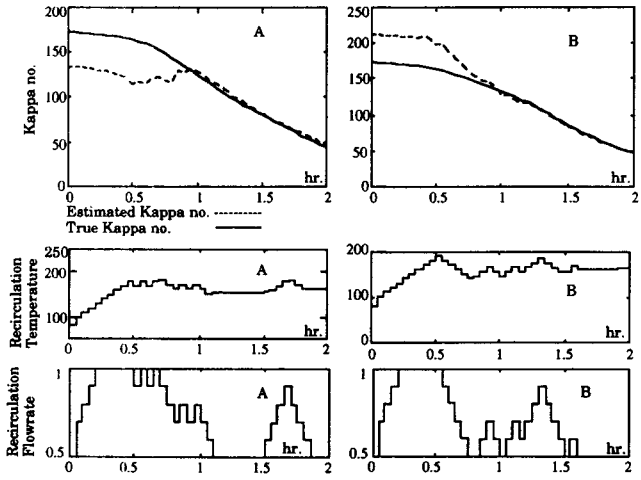

Figure 5. Case study 1C with both types of initial state errors, closed-loop plot of estimated and true Kappa number profiles when all four measurements are used.

A) Type-1 initial state errors; B) type-2 initial state errors.

Case study 2

In this study, the model parameters are perturbed to various degrees to check the robustness of the state estimation algorithm to model-plant mismatch. This is necessary because often

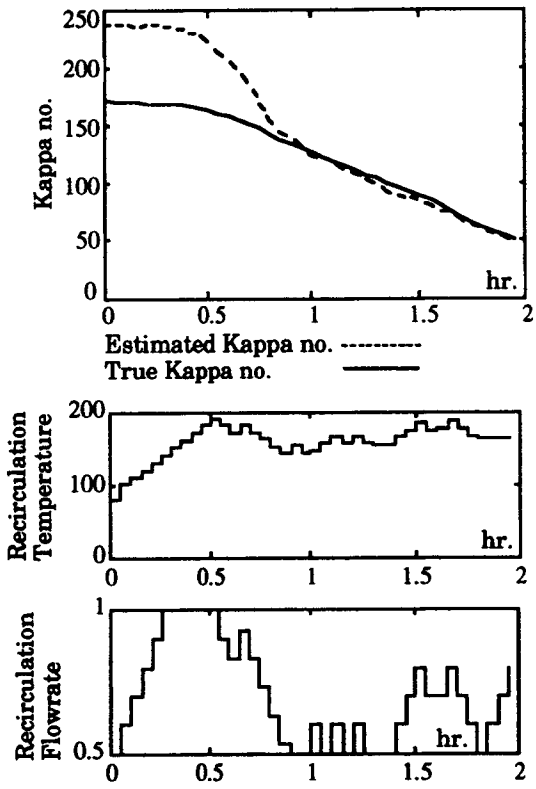

Figure 7. Case study 1E with type-2 initial state errors, effect of high error in initial state estimates on closed-loop profiles of the estimated and true Kappa number.

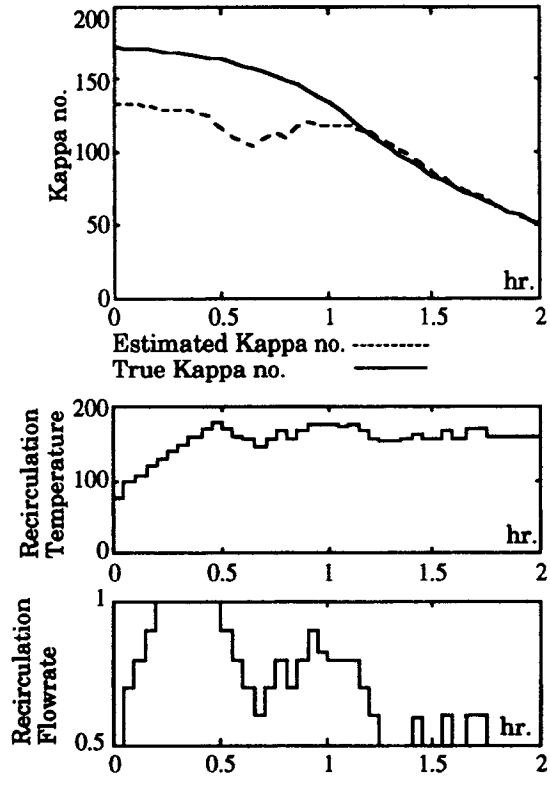

Figure 8. Case study 2, the effect of +100% error in A_{1_i} and type-1 initial state errors on closed-loop profiles of the estimated and true Kappa number.

chosen model parameters are not exactly equal to the true parameters, and such discrepancies can influence the performance of the controller. Furthermore, while the controller works well despite a large amount of errors in some parameters, it may fail when only a small amount of error is present in other parameters.

Frequency factors and activation energies of various reactions are important model parameters of the pulp digester model. Recalling the expressions for the reaction rates from Appendix A, the first rate constant k_{1_i} involves A_{1_i} and E_{1_i} as the frequency factor and activation energy, A_{2_i} and E_{2_i} represent the same quantities for the second rate constant k_{2_i}. Since the number of wood components is five, there are ten activation energies and ten frequency factors, leading to 20 model pa-

Table 5. Accuracy of Model Parameters; Type of Model Errors and Initial State Estimate Errors Leading to Poor Kappa Number Estimate

Importance of Model Accuracy	Parameters	Values of Parameters*	Types of Initial State Errors
high	E_{1_2} = first activation energy of second wood component	lower	type 1
high	E_{1_2} = first activation energy of second wood component	higher	type 2
high	E_{2_2} = second activation energy of second wood component	lower	type 1
high	M_{1_i} & M_{2_i} = constants in mass-transfer coeff. equation	higher	type 1
high	M_{1_i} & M_{2_i} = constants in mass-transfer coeff. equation	lower	type 2
medium	A_{1_2} = first frequency factor of second wood component	higher	type 1
medium	A_{1_2} = first frequency factor of second wood component	lower	type 2
medium	E_{2_1} = second activation energy of first wood component	higher	type 2
low	A_{2_1} = second frequency factor of first wood component	lower	type 2

* Based on expected deviations in parameter estimates from their true values.

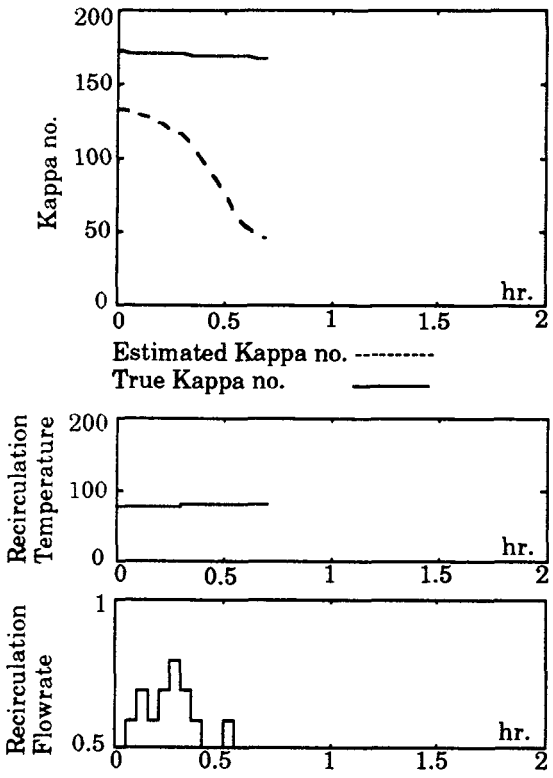

Figure 9. Case study 2, the effect of −50% error in E_{2_2} with type-1 initial state errors on closed-loop profiles of the estimated and true Kappa number.

rameters. Other model parameters, whose values may be uncertain, are orders of reaction with respect to NaOH (a) and NaSH (b), stoichiometric consumption rates of NaOH ($S_{c_{3,i}}$) and NaSH ($S_{c_{4,i}}$), constants in the mass-transfer coefficient equation of the liquor components (M_{1_i} and M_{2_i}), heat of reaction (ΔH_i) and specific heat (Cp_{w_i}) of the wood components. Because the data on M_{1_i}, M_{2_i}, ΔH_i, and Cp_{w_i} for various components (i) were unavailable to us, we assumed that the values for these parameters are the same for all the components. Therefore, a total of 36 different model parameters are considered in this case study.

To bring out the maximum effect of model errors when coupled with initial state estimate errors, we have simulated the worst combinations of such errors. One of such worst error combinations is when we have the type-1 initial state errors (in this case, the estimated Kappa number is lower than the true value) and model errors predict the reaction rate to be faster than the true rate, so that the estimated Kappa number fall more rapidly than the true value. Therefore, in the absence of any filtering, the estimated Kappa number will continue to diverge away from the true Kappa number. Faster reaction is predicted when the model parameters differ from its true values such as higher frequency factors, lower activation energies, higher reaction orders, lower stoichiometric coefficients, higher mass-transfer coefficients, and higher heat of reaction. An opposite scenario occurs when the model indicates the reaction rate to be slower than the true rate, and there exist type-2 initial state errors.

We simulated the effect of the error in each parameter when the initial state errors are present as stated above and found that these parameters can be arranged in the order of importance, based on their effect on the controller performance. Our observation is shown in Table 5. For combinations of model and initial state errors not listed in this table, the estimated and true values were found to approach each other closely, even when parametric errors as large as +100% or −50% (within physical limits) were present.

Figure 8 shows that, even in the presence of +100% error in the parameter A_{1_1} with the type-1 initial errors, the closed-loop performance remains unaffected. On the other hand, Figure 9 indicates how the closed-loop performance is adversely affected when −50% error in the parameter E_{2_2} occurs with the type-1 initial errors. In this case, estimated Kappa number acquires the target value much ahead of the given batch time, when no significant change in the true Kappa number occurs. In other words, compared to A_{1_1}, error in E_{2_2} has a much more pronounced effect on the delignification rate and thus more degrading effect on the Kappa number estimate.

This case study clearly suggests that we must account for the potential model errors in our design by incorporating either on-line or frequent off-line identification of the important model parameters.

Conclusions

The application of the extended-Kalman-filter-based NLMPC to batch pulp digesters has been discussed. The Extended Kalman filter and the MPC controller, combined with new liquor analyzers, can significantly improve control of pulp digesters, provided that we can identify some critical model parameters with reasonable accuracy. The extended Kalman filter utilizing various liquor measurements shows a good convergence property, even when the state errors and disturbances are undermodeled.

While the case studies indicated great potential for using model-based control for pulp digesters, they also hinted the need for on-line estimation of some important model parameters. Our preliminary experience with the extended Kalman filter for simultaneous state/parameter estimation has not been very positive. This problem needs to be fully resolved before the technique can be taken to industrial settings. We are investigating ways of alleviating this difficulty: 1. potential benefits of using more computationally intensive, yet powerful, nonlinear-programming-based estimation techniques, such as the receding horizon estimation proposed by Lee et al. (1992); 2. reducing the order and number of parameters for the batch digester model by lumping together some of less important physicochemical phenomena. In conjunction with these efforts, experimental study of a bench-scale batch digester is also being undertaken at Auburn University.

Acknowledgment

Financial support of the Pulp and Paper Research and Education Center (PPREC) at Auburn University is gratefully acknowledged.

Notation

a, b = reaction orders (for second term in the expression of R_i) of NaOH and NaSH, respectively
A = surface area of such mass transfer, m^2

A_{1_i} = 1st frequency factor of component i, same units as k_{1_i}
A_{2_i} = 2nd frequency factor of component i, same units as k_{2_i}
C_{e_i} = concentration of ith component in entrapped liquor, kg/m^3
C_{f_i} = concentration of ith component in free liquor, kg/m^3
Cp_{e_i} = specific heat of ith component in entrapped liquor, kcal/kg·K
Cp_{f_i} = specific heat of ith component in free liquor, kcal/kg·K
Cp_{r_i} = specific heat of ith component in recirculation liquor, kcal/kg·K
Cp_{w_i} = specific heat of ith component in wood, kcal/kg·K
C_{r_i} = concentration of ith component in the recirculation (assumed to be equal to C_{f_i}), kg/m^3
E_{1_i} = 1st activation energy of component i, kcal/mol
E_{2_i} = 2nd activation energy of component i, kcal/mol
F_r = recirculation flow rate, m^3/h
G_i = total rate of generation of ith entrapped liquor component (positive for Lignin and total solid, and negative for NaOH and NaSH), kg/h·kg dry wood mass
ΔH_i = heat of reaction, (kcal/kg of ith wood component disappearing)
k_{1_i} = 1st rate constant of component i, h^{-1} (kg/m^3)$^{-1}$
k_{2_i} = 2nd rate constant of component i, h^{-1} (kg/m^3)$^{-a-b}$
K_t = total heat capacity, kcal/K
M_i = mass-transfer coefficient of ith component between entrapped and free liquor phases, m/h
M_w = total mass of dry wood, kg
M_{1_i} = empirical constant, m/h
M_{2_i} = empirical constant, m/h·K
N_e = number of components entrapped in liquor (including water)
N_f = number of components in free liquor (including water)
N_w = number of components in wood
R = ideal gas constant, kcal/mol·K
R_i = reaction rate of ith component based on wood mass, mass fraction/h
$S_{c_{i,j}}$ = stoichiometric coefficient of ith entrapped liquor component, per unit mass of jth wood component disappearing by reaction, kg/kg
T = temperature, K
T_r = recirculation temperature, K
V_e = total volume of entrapped liquor, m^3
V_f = total volume of free liquor, m^3
X_i = concentration of ith component in wood, mass fraction
X_{u_i} = unreactable concentration of wood component i, mass fraction

Literature Cited

Armstrong, M. K., "Statistical Process Control of Digester Permanganate and Kappa Numbers: Closing the Loop with SPC," *Tappi J.*, **74**, 244 (1991).

Beigler, L. T., and J. E. Cuthrell, "On the Optimization of Differential-Algebraic Process Systems," *AIChE J.*, **33**(8), 1257 (1987).

Bellgardt, K. H., W. Kuhlmann, H. D. Meyer, K. Schugeri, and M. Thoma, "Application of an Extended Kalman Filter for State Estimation of a Yeast Fermentation," *IEEE Proc.*, **133.D**(5), 226 (1986).

Bequette, B. W., "Nonlinear Control of Chemical Processes: A Review," *Ind. Eng. Chem. Res.*, **30**, 1391 (1991).

Chari, N. C. S., "Integrated Control System Approach for Batch Digester Control," *Tappi J.*, **56**(7), 65 (1973).

Corcoran, C. A., and S. C. Rutan, "Correction for Temperature Variations in Kinetic Methods of Analysis with Extended Kalman Filter," *Anal. Chem.*, **60**, 1146 (1988).

Cox, H., "On the Estimation of State Variables and Parameters for Noisy Dynamic Systems," *IEEE Trans. Autom. Control*, **23**, 149 (1987b).

Dumont, G. A., "Application of Advanced Control Methods in the Pulp and Paper Industry—A Survey," *Automatica*, **22**(2), 143 (1986).

Garcia, C. E., "Quadratic/Dynamic Matrix Control of Nonlinear Processes: An Application to a Batch Process," AIChE Meeting, San Francisco (1984).

Gattu, G., and E. Zafiriou, "Nonlinear Quadratic Dynamic Matrix Control with State Estimation," *Ind. Eng. Chem. Res.*, **31**(4), 1096 (1992).

Hatton, J. V., "Application of Empirical Equations to Kraft Process Control," *Tappi J.*, **56**(8), 108 (1973).

Kerr, A. J., and J. M. Uprichard, "The Kinetics of Kraft Pulping—Refinement of a Mathematical Model," *Appita*, **30**(1), 48 (1976).

Kopp, R. E., and R. J. Oxford, "Linear Regression Applied to System Identification and Adaptive Control System," *AIAA J.*, **1**(10), 2300 (1963).

Lee, J. H., and N. L. Ricker, "Extended Kalman Filter Based Nonlinear Model Predictive Control," *Proc. of Amer. Control Conf.*, San Francisco (1993).

Lee, J. H., J. B. Rawlings, and D. Robertson, "Constrained State Estimation and Its Application to Model Predictive Control," AIChE Meeting, Miami Beach, FL (1992).

Myers, M. A., and R. H. Luecke, "Process Control Applications of an Extended Kalman Filter Algorithm," *Comp. & Chem. Eng.*, **15**(12), 853 (1991).

Poulonis, M. A., and A. Krishnagopalan, "Adaptive Inferential Control of Kraft Batch Digesters as Based on Pulping Liquor Analysis," *Tappi J.*, **74**, 169 (1991).

Rawlings, J. B., A. A. Patwardhan, and J. B. Edgar, "Nonlinear Model Predictve Control," *Chem. Eng. Commun.*, **87**, 123 (1990).

Venkateswarlu, C., and K. Gangiah, "Dynamic Modelling and Optimal State Estimation Using Extended Kalman Filter for a Kraft Pulping Digester," *Ind. Eng. Chem. Res.*, **31**, 848 (1992).

Wells, C. H., "Effective Alkali Sensors for Batch Digester Control," *Tappi J.*, **73**, 181 (1990).

Wells, C. H., "Application of Modern Estimation and Identification Techniques to Chemical Processes," *AIChE J.*, **17**(4), 966 (1971).

Williams, T. J., and C. C. Smith, "A Dynamic Model of a Kamyr Digester and Its Application to Pulp Washing and Pulping Reaction Control," *Modelling Control of Kraft Prod. Sys., Pulp Prod., Chem. Recovery, Energy Conservation Proc.*, ISA Symp., Pittsburgh (1975).

Williams, T. J., C. C. Smith, T. Christensen, and L. F. Albright, "Modelling of Batch Kraft Pulping and of Kamyr Digesters," *Pulp and Paper Canada*, **85**(8), 55 (1984).

Williams, T. J., T. Christiansen, and L. F. Albright, "A Mathematical Model of the Kraft Pulping Process: 1 and 2," Purdue Laboratory for Applied Industrial Control, Report No. 129, 41, 229 (1982).

Williams, T. J., L. F. Albright, and G. B. Stark, "Parameter Identification in the On-Line Simulation of the Operation of the Kamyr Digester," Purdue Laboratory for Applied Industrial Control, Report No. 151, 4 (1987).

Appendix A: Model Equations for Batch Pulp Digester

Equation A1 comprises various wood components: high-reactive lignin, low-reactive lignin, cellulose, galactoglucomannan (hemicellulose 1) and araboxylan (hemicellulose 2). Equation A2 or A3 comprises various entrapped or free liquor components: total dissolved lignin, dissolved solid (except for lignin coming out of wood), NaOH and NaSH. For details about this model including various assumptions see Williams and Smith (1975) and Williams et al. (1982, 1984, 1987). The model equations are:

$$\frac{dX_i}{dt} = R_i \quad (1 \le i \le 5) \tag{A1}$$

$$V_e \frac{dC_{e_i}}{dt} = M_w G_i - M_i A (C_{e_i} - C_{f_i}) \quad (1 \le i \le 4) \tag{A2}$$

$$V_f \frac{dC_{f_i}}{dt} = M_i A (C_{e_i} - C_{f_i}) - F_r (C_{f_i} - C_{r_i}) \quad (1 \le i \le 4) \tag{A3}$$

$$K_t\frac{dT}{dt}=M_w\sum_{i=1}^{N_w}(-R_i)(-\Delta H_i)+F_r\sum_{i=1}^{N_f+1}C_{r_i}Cp_{r_i}(T_r-T) \quad \text{(A4)}$$

$$R_i=-[k_{1_i}C_{e_3}+k_{2_i}C_{e_3}^aC_{e_4}^b](X_i-X_{u_i}) \quad \text{(A5)}$$

$$k_{1_i}=A_{1_i}e^{E_{1_i}/RT} \quad \text{(A6)}$$

$$k_{2_i}=A_{2_i}e^{E_{2_i}/RT} \quad \text{(A7)}$$

$$\text{Lignin: } G_1=-\sum_{j=1}^{2}R_j \quad \text{(A8)}$$

$$\text{Solid: } G_2=-\sum_{j=3}^{5}R_j \quad \text{(A9)}$$

$$\text{NaOH: } G_3=\sum_{j=1}^{5}S_{c_{3_j}}R_j \quad \text{(A10)}$$

$$\text{NaSH: } G_4=\sum_{j=1}^{5}S_{c_{4_j}}R_j \quad \text{(A11)}$$

$$M_i=M_{1_i}+M_{2_i}T \quad \text{(A12)}$$

$$K_t=\left[M_w\sum_{i=1}^{N_w}Cp_{w_i}X_i+V_e\sum_{i=1}^{N_e+1}Cp_{e_i}C_{e_i}+V_f\sum_{i=1}^{N_f+1}Cp_{f_i}C_{f_i}\right] \quad \text{(A13)}$$

Appendix B

Model parameters for EKF

Matrices A_{k-1} and B_{k-1}^d in Eqs. 25 are obtained through affine linear approximation of the nonlinear model (Eq. B1) with respect to $x_{k-1}=x_{k-1|k-1}$ and $d_{k-1}=C^wx_{k-1|k-1}^w$ and are defined as:

$$A_{k-1}=\exp(\tilde{A}_{k-1}T_s) \quad \text{(B1)}$$

$$B_{k-1}^d=\int_0^{T_s}\exp(\tilde{A}_{k-1}\tau)d\tau\cdot\tilde{B}_{k-1|k-1} \quad \text{(B2)}$$

$$\tilde{A}_{k-1}=\left.\frac{\partial f(x,u,d)}{\partial x}\right|_{x=x_{k-1|k-1},u=u_{k-1},d=C^wx_{k-1|k-1}^w} \quad \text{(B3)}$$

$$\tilde{B}_{k-1}=\left.\frac{\partial f(x,u,d)}{\partial d}\right|_{x=x_{k-1|k-1},u=u_{k-1},d=C^wx_{k-1|k-1}^w} \quad \text{(B4)}$$

C_k and C_k^d in Eq. 29 are obtained through linearization of output Eq. B3 with respect to the estimates $x_k=x_{k|k-1}$ and $d_k=C^wx_{k|k-1}^w$ and are defined as:

$$C_k=\left.\frac{\partial g(x,d)}{\partial x}\right|_{x=x_{k|k-1},d=C^wx_{k|k-1}^w} \quad \text{(B5)}$$

$$C_k^d=\left.\frac{\partial g(x,d)}{\partial d}\right|_{x=x_{k|k-1},d=C^wx_{k|k-1}^w} \quad \text{(B6)}$$

Model parameters for MPC prediction equation

After measurement correction has been done at time k, the model is linearized as:

$$\begin{bmatrix}x_{k+1}\\x_{k+1}^w\end{bmatrix}\approx\begin{bmatrix}f_{T_s}(x_{k|k},u_{k-1},C^wx_{k|k}^w)\\A^wx_{k|k}^w\end{bmatrix}+\begin{bmatrix}\mathfrak{B}_k^u\\0\end{bmatrix}(u_k-u_{k-1})+\begin{bmatrix}\mathfrak{A}_k&\mathfrak{B}_k^dC^w\\0&A^w\end{bmatrix}\begin{bmatrix}x_k-x_{k|k}\\x_k^w-x_{k|k}^w\end{bmatrix}+\begin{bmatrix}0\\B^w\end{bmatrix}w_k \quad \text{(B7)}$$

with various constant matrices are obtained through linearization of dynamic model (Eqs. B1-B3) with respect to ($x_{k|k}$, u_{k-1} and $d_{k|k}=C^wx_{k|k}^w$) as:

$$\mathfrak{A}_k=\exp(\tilde{\mathfrak{A}}_kT_s) \quad \text{(B8)}$$

$$\mathfrak{B}_k^u=\int_0^{T_s}\exp(\tilde{\mathfrak{A}}_k\tau)d\tau\cdot\tilde{\mathfrak{B}}_k^u \quad \text{(B9)}$$

$$\mathfrak{B}_k^d=\int_0^{T_s}\exp(\tilde{\mathfrak{A}}_k\tau)d\tau\cdot\tilde{\mathfrak{B}}_k^d \quad \text{(B10)}$$

$$\tilde{\mathfrak{A}}_k=\left.\frac{\partial f(x,u,d)}{\partial x}\right|_{x=x_{k|k},u=u_{k-1},d=C^wx_{k|k}^w} \quad \text{(B11)}$$

$$\tilde{\mathfrak{B}}_k^u=\left.\frac{\partial f(x,u,d)}{\partial u}\right|_{x=x_{k|k},u=u_{k-1},d=C^wx_{k|k}^w} \quad \text{(B12)}$$

$$\tilde{\mathfrak{B}}_k^d=\left.\frac{\partial f(x,u,d)}{\partial d}\right|_{x=x_{k|k},u=u_{k-1},d=C^wx_{k|k}^w} \quad \text{(B13)}$$

Note that, since expectations of $x_k-x_{k|k}$ and w_k are both zero,

$$\begin{bmatrix}x_{k+1|k}\\x_{k+1|k}^w\end{bmatrix}\approx\begin{bmatrix}f_{T_s}(x_{k|k},u_{k-1},C^wx_{k|k}^w)\\A^wx_{k|k}^w\end{bmatrix}+\begin{bmatrix}\mathfrak{B}_k^u\\0\end{bmatrix}(u_k-u_{k-1}) \quad \text{(B14)}$$

Now, extending this idea to p future time steps, one can develop the multistep prediction equation of controlled variables (y^c) as:

$$\begin{aligned}\mathcal{Y}_{k+1|k}&=\mathcal{S}_k^x(x_{k|k},u_{k-1},x_{k|k}^w)+\mathcal{S}_k^w x_{k|k}^w+\mathcal{S}_k^{\mathcal{U}}\Delta\mathcal{U}_k\\&\triangleq\mathcal{Y}_{k+1|k}^0+\mathcal{S}_k^{\mathcal{U}}\Delta\mathcal{U}_k\end{aligned} \quad \text{(B15)}$$

where,

$$\mathcal{Y}_{k+1|k}=\begin{bmatrix}y_{k+1|k}^c\\y_{k+2|k}^c\\\vdots\\y_{k+p|k}^c\end{bmatrix};\quad\Delta\mathcal{U}_k=\begin{bmatrix}\Delta u_k\\\Delta u_{k+1}\\\vdots\\\Delta u_{k+p-1}\end{bmatrix} \quad \text{(B16)}$$

$$\mathcal{S}_k^x(x_{k|k}, u_{k-1}, x_{k|k}^w) = \begin{bmatrix} Hf_{T_s}(x_{k|k}, u_{k-1}, C^w x_{k|k}^w) \\ Hf_{2.T_s}(x_{k|k}, u_{k-1}, C^w (A_w)^i x_{k|k}^w | 0 \le i \le 1) \\ \vdots \\ Hf_{p.T_s}(x_{k|k}, u_{k-1}, C^w (A_w)^i x_{k|k}^w | 0 \le i \le p) \end{bmatrix} \tag{B17}$$

$$\mathcal{S}_k^w = \begin{bmatrix} H^d C^w A^w \\ H^d C^w (A^w)^2 \\ \vdots \\ H^d C^w (A^w)^p \end{bmatrix} \tag{B18}$$

$$\mathcal{S}_k^u = \begin{bmatrix} H\mathcal{B}_k^u & 0 & \cdots & 0 \\ H(\mathcal{A}_k \mathcal{B}_k^u + \mathcal{B}_k^u) & H\mathcal{B}_k^u & \cdots & 0 \\ \vdots & \vdots & \ddots & \vdots \\ \Sigma_{i=0}^{p-1} H\mathcal{A}_k^i \mathcal{B}_k^u & \cdots & \cdots & H_k \mathcal{B}_k^u \end{bmatrix} \tag{B19}$$

$f_{p.T_s}[x_{k|k}, u_{k-1}, C^w (A^w)^i x_{k|k}^w |_{0 \le i \le p-1}]$ represents the terminal state values resulting from integrating the nonlinear differential equation $\dot{x} = f(x, u, d)$ for p sampling intervals with initial condition $x_{k|k}$, constant input $u = u_{k-1}$ and piecewise constant input d taking the value of $C^w (A^w)^i x_{k|k}^w$ during the time interval $[k+i, k+i+1]$.

Manuscript received Dec. 18, 1992, and revision received May 3, 1993.